Available online at www.sciencedirect.com
SCIENCE DIRECT®
Journal of Power Sources 145 (2005) 470–476
JOURNAL OF POWER SOURCES
www.elsevier.com/locate/jpowsour

Transport phenomena and performance limits in polymeric electrolyte membrane fuel cells

A. Serrafero, E. Arato *, P. Costa

Department of Environmental Engineering, University of Genoa, via Opera Pia 15, 16145 Genoa, Italy

Accepted 10 February 2005
Available online 28 April 2005

Abstract

In polymeric electrolyte fuel cells the hydration level of the perfluosulphonic membrane used as electrolyte is a very important parameter for proton conductivity. Only an accurate local description of the hydration condition of the membrane allows a reliable prediction of cell performance.

In this work we refer to the development of a detailed model of a polymeric fuel cell that takes into account a local integration of mass and charge transport equations throughout the membrane and the mass, energy (gas and solid) and momentum balances on the plane of the cell. The calculation of all the voltage losses and the temperature and humidity conditions on both the cathodic and the anodic sides helps in understanding how to avoid undesirable working conditions.

Of particular interest is the possibility of simulating different feeding systems (co-flow, counter-flow, cross-flow) as well as different flow fields (conventional, serpentine, interdigitated).

The modelling results for polymeric fuel cells, fed by hydrogen or methanol, are presented in terms of characteristic curves for different flow geometries and operative parameters and are compared with literature data.

Keywords: Transport phenomena; Modelling; Polymeric fuel cells; Gas flow mode

1. Introduction

Among the fuel cells working at low temperature, proton exchange membrane fuel cells (PEMFCs) are efficient and environmentally friendly electrical generators that are being developed for both stationary and mobile applications [1]. They are characterised by the use of a perfluosulphonic membrane (usually Nafion®) as electrolyte. This type of membrane is a good proton conductor, due to the fact that the sulphonic groups easily dissociate into SO_3^- (fixed charge) and H^+ (mobile charge) in the presence of water. In this way the membrane performs the dual functions of transferring H^+ from the anode to the cathode and separating the reactants, as it is impermeable to gas.

As mentioned above, the hydration level is an important parameter for proton conductivity and it is specifically for this reason that this phenomenon can be accurately described using a local model. Membrane hydration is strongly related to the humidity of the reactant gases which are usually humidified by bubbling through high-temperature water columns, before being fed to the cell. Water is also involved in the cell reactions and it is produced at the cathode:

$$H_2 \rightarrow 2H^+ + 2e^- \quad \text{(anode)}$$

$$2H^+ + 1/2\, O_2 + 2e^- \rightarrow H_2O \quad \text{(cathode)}$$

$$H_2 + 1/2\, O_2 \rightarrow H_2O \quad \text{(overall reaction)}$$

Another matter of major interest is the control of the temperature. In fact, the membrane may suffer irreversible damage at temperatures around 130 °C (the vitreous transition

* Corresponding author. Tel.: +39 0103532926; fax: +39 0103532589.
E-mail address: betta@diam.unige.it (E. Arato).

0378-7753/$ – see front matter © 2005 Elsevier B.V. All rights reserved.
doi:10.1016/j.jpowsour.2005.02.039

Nomenclature

C	concentration (mol m^{-3})
C_p	specific heat (J mol^{-1} K^{-1})
d	cell channels height (m)
D	diffusivity in the membrane (m^2 s^{-1})
F	Faraday's constant (C mol^{-1})
h	heat transfer coefficient (J s^{-1} m^{-2} K^{-1})
ΔH	enthalpy of reaction (J mol^{-1})
J	current density (A m^{-2})
k	heat conductivity (W m^{-1} K^{-1})
K	constant in Table 1
n	molar flow rate (mol m^{-2} s^{-1})
P	total pressure (Pa)
R	gas constant (J mol^{-1} K^{-1})
r	reaction rate (mol m^{-2} s^{-1})
s	layer thickness (m)
S	effective interface surface gas/solid (m^2 m^{-2})
T	temperature (K)
u	gas velocity (m s^{-1})
v	molar volume (m^3 mol^{-1})
V	voltage (V)
x	cell co-ordinate (m)
z	electric charge, dimensionless

Greek letters

η	overpotential
λ	membrane hydration, i.e. the ratio H_2O/SO_3^- in membrane, dimensionless
μ	gas viscosity (Pa s)
ν	stoichiometric coefficient, dimensionless
χ_{ip}, χ_{iv}	non ideality coefficients in Eq. (2), dimensionless

Subscripts

i	component
j	reaction
k	anodic or cathodic co-ordinate
n	cell unit component
r	refrigerant
s	solid

temperature of Nafion®). For this reason the cell is usually fed with a cooling liquid (usually water) to contain the temperature peaks that can damage the cell.

However, it has been noted that low temperatures may provoke another significant phenomenon: water flooding the cathode and blocking the catalyst pores, producing a diffusion barrier.

Recently, direct methanol fuel cells (DMFCs) have been shown to be an attractive option for electrochemical power [2,3]: the main difference from PEMFCs being that the fuel is more or less a concentrated methanol solution. In this case the water acts as a carrier for the methanol, and also serves

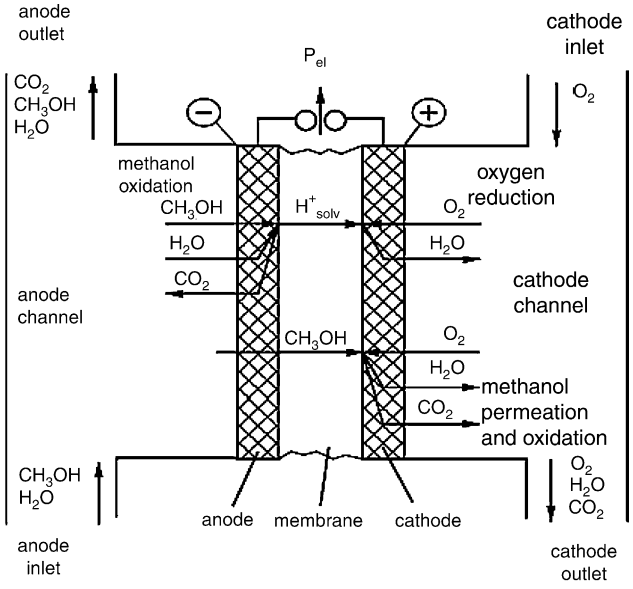

Fig. 1. Schematisation of a DMFC.

to effectively remove excess heat [3] and, obviously, control the membrane hydration level (see Fig. 1).

The main advantage of this type of cell is the easy storage of the high energy density liquid fuel [4]. In the cell, methanol is oxidised to carbon dioxide at the anode and oxygen is reduced to water at the cathode according to the following scheme:

$$CH_3OH + H_2O \rightarrow CO_2 + 6\,H^+ + 6e^- \quad \text{(anode)}$$

$$3/2\,O_2 + 6\,H^+ + 6e^- \rightarrow 3\,H_2O \quad \text{(cathode)}$$

$$CH_3OH + 3/2\,O_2 \rightarrow CO_2 + 2\,H_2O \quad \text{(overall reaction)}$$

However, there are two main obstacles to the utilisation of DMFCs. One is low performance (low power density) due to the poor kinetics of the oxidation reaction of methanol in the anode. In fact, in the case of methanol, six electrons must be exchanged for complete oxidation and consequently the oxidation kinetics are inherently slower, as a result of intermediates formed during methanol oxidation.

The other is a crossover phenomenon: methanol fed to the anode penetrates the polymer electrolyte membrane and causes a decrease in the cathodic potential and energy efficiency [5]. The methanol molecules that have reached the cathodic compartment readily chemisorb on the electrode surface with subsequent oxidation to CO_2: this causes a "mixed potential", which decreases the cell potential [6]. Different from PEMFCs, the methanol component crosses the membrane because, having low activation energy, only a small part is converted on the electrocatalyst, while the remainder is free to migrate to the cathode due to electroosmosis and the concentration difference.

Recently [7] the development of DMFCs has led to the possibility of using two different feed systems: liquid feed

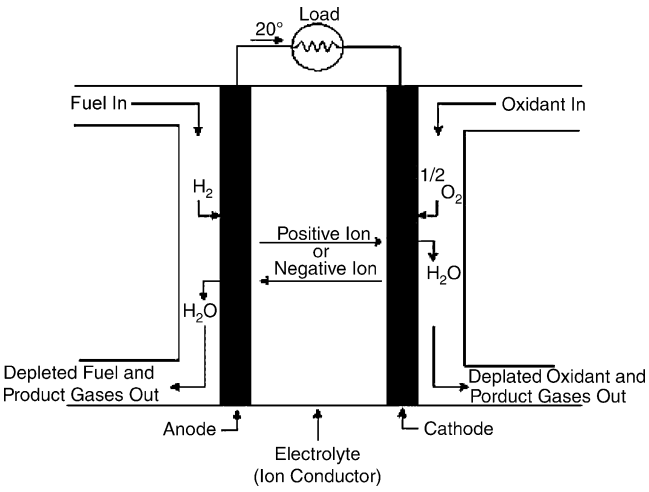

Fig. 2. Functional scheme of a PEMFC.

direct methanol fuel cell (LFDMFC) and vapour feed direct methanol fuel cell (VFDMFC). The main advantages of LFDMFCs are the good hydration of the membrane and the higher thermal capacity for cooling and heat transfer, while the disadvantages are the existence of methanol and water vapour in the carbon dioxide exhaust gas and the temperature limitations of liquid operation.

The main advantages of VFDMFCs are superior performance and higher methanol fuel conversion while the disadvantages are possible problems relating to membrane dehydration and large amounts of water and carbon dioxide in the exhaust gas.

2. Model

The model developed for the present study schematised every local portion of the positive electrode–electrolyte–negative electrode (PEN) along the plane of the cell, subdividing it ideally into five regions (Fig. 2): anodic flow channel, anodic electrocatalyst, membrane, cathodic electrocatalyst and cathodic flow channel; a number of cells superimposed and electrically connected in series to the others by bipolar plates was then considered in order to simulate the stack.

2.1. Local balances

The model includes the local balance equations for a two-dimensional domain. The balances of mass, energy and momentum for the gases and the energy balance of the solid and refrigerant are considered. In Table 1 all the equations applied to each cell unit are presented. The complete theory is described in detail in [8,9].

2.2. Local kinetics

The most critical point for the model is the formulation of the local kinetics, which has to be determined for every point on the plane of the cell. In general, each type of cell has its own particular thermodynamic potential ΔE^{Term}, calculable from the Nernst equation, which is dependent on the temperature, pressure and composition of the feed, and penalized by a number of losses due to irreversible phenomena.

More specifically, the cell potential of polymeric fuel cells can be estimated in the following manner:

$$\Delta V = \Delta E^{\text{Term}} - \eta^{\text{electrode}} - \eta^{\text{ocv}} - \eta^{\text{diff}} - \eta^{\text{memb}} \quad (1)$$

In the case of PEMFCs, the second term represents the losses due to the activation overpotential of the two electrochemical reactions: it has been noted that the literature states that the anodic overpotential is less important for much longer than the cathodic, and the latter can be expressed by Tafel's Law [10]. In DMFCs the losses due to the activation of both the reactions (anodic and cathodic ones) are important and are calculated from an extensions of Tafel's Law [11].

The third term combines phenomena that also occur in open-circuit performance in polymeric fuel cells. In PEMFCs this represents the contribution due to parasitic phenomena: there is the possibility that the reactants will cross the membrane and initiate undesirable electrochemical reactions that will lower the cell tension. The experimental literature data show a constant contribution to this loss, the value of which can vary, however, according to the case being studied [12,13]. In DMFCs this represents the losses due to methanol crossover, a particular phenomenon found in open circuits. Just as water molecules are transported from the anode to the cathode by diffusion and electroosmotic phenomena, methanol passes through the membrane to reach the

Table 1
Summary of the model equations

Mass balances	Gas	$\frac{\partial n_i}{\partial x_k} = r_i$ where $r_i = \sum_j \nu_{i,j} r_j$ and $r_j = J/n_j F$
Energy balances	Gas	$\sum_i n_i C_{\text{p}_i} \frac{\partial T_k}{\partial x_k} = \sum_i \frac{\partial n_i}{\partial x_k} \int_{T_k}^{T_s} C_{\text{p}_i}\, \text{d}T_k + S_k h_k (T_s - T_k)$
	Refrigerant	$C_{\text{p}_r} \frac{\partial T_r}{\partial x_r} = S_r h_r (T_s - T_r)$
	Solid	$\sum_k S_k h_k (T_s - T_k) = Q_{\text{cond}} + Q_{\text{reaz}}$ where $Q_{\text{cond}} = \sum_n (s_n k_n) \left(\sum_k \frac{\partial^2 T}{\partial x_k^2} \right)$ and $Q_{\text{reaz}} = \sum_j r_j \Delta H_j - VJ$
Momentum balances	Gas	$\frac{\partial P_k}{\partial x_k} = -K_k \frac{\mu_k v_k}{d^2}$

cathode and react with the oxygen to create a "mixed potential" that reduces the cell potential [14].

The fourth term represents the loss voltage due to the diffusion of the reactants towards the electrode: this is important for high current density; that is, when the imposed current approaches the limit one and the characteristic curve shows a "knee-bend" trend [10]. On the contrary, in DMFCs the resistance due to the diffusion of the reagents is not considered in the literature and so has not been considered in the model up to now.

The last term, the membrane voltage loss, is due to the resistance of the membrane to the passage of H^+. In every case the loss due to membrane resistance is very significant if not controlling. This term, will be more fully described below.

2.3. Membrane

As already stated, in the polymeric membrane fuel cell, the ionic conduction takes place under significantly different conditions to those that occur in a normal electrolytic solution:

- the positive charges are mobile, while the negative ones are an integral part of the solid structure of the membrane;
- the positive charges do not move like free protons, but like solvated ones, with the flow ratio between protons and water about 2.3;
- the flow of positive charges provokes the flow of the solvent, which is also influenced by the non-uniform hydration of the membrane and the pressure gradient.

A further discussion of the transport mechanisms will help in understanding the behaviour of polymeric membranes in commercial use. In particular, the model takes into consideration the fact that the protons migrate in solvated form and that the fluxes that cross the membrane depend on the following driving forces:

- concentration gradients in the water phase, which induce diffusion fluxes of single components;
- electrical potential gradients, which make the positive ions migrate, but which are also unbalanced global forces;
- pressure gradients, which act on all the fluid;
- gradients due to the degree of membrane humidification, linked to capillary forces and therefore comparable to an additional pressure gradient, and also acting on all the fluid.

On the basis of these considerations, the flux of the species, when concentration, pressure and electric potential gradients occur, can be written following equation [15]:

$$\underline{n_i} = -D_i \left(\nabla C_i + \chi_{\text{ip}} \frac{C_i v_i}{RT} \nabla P + z_i C_i \chi_{\text{iv}} \frac{F}{RT} \nabla V \right) \qquad (2)$$

This is substantially the Nernst–Planck equation, which is assumed to hold for the entire membrane thickness: non-linearity effects due to membrane structure and variable local hydration can be taken into account by means of non-constant diffusivity coefficients $D_i(\lambda)$ and correction factors $\chi_{\text{i.p.}}$, $\chi_{\text{i.v.}}$. We have demonstrated [15] that with opportune simplification it is possible to obtain reliable analytical expressions of the fluxes. The accuracy is comparable with that of the numerical and iterative methods, while the calculation time is substantially lower and there is no convergence uncertainty.

This analysis is valid for PEMFCs and DMFCs: for the latter the calculation of the methanol flux across the membrane is added (a phenomenon to be minimised as it represents one of the cell potential losses). With regard to this, it is possible to state that the available data on membrane humidification equilibria and the "co-ordination number" (average number of methanol molecules that are bound to a single proton) for methanol are considerably less than for water.

3. Model solution

The model, in Fortran language, provides the integration of the local balance equations of mass, energy and momentum on the cell plane by using the finite difference method. The requested input data are relative to the technical data of the membrane and the component materials, and the operating conditions, that is the temperature and composition of the reactants, the operative pressure, the temperature of the refrigerant and the electrical current (or cell voltage) imposed.

The output data supply the maps (always on the cell plane) of solid, gas and refrigerant fluid temperatures, gas compositions, pressure, current density, humidity and the characteristic curve of the cell. The resolution times are of the order of 10s of seconds.

The model provides several calculation options: the most significant being the possibility of choosing between different types of flow geometry that can be grouped in two categories.

The first is based on the pathway really followed by the single gas (anodic and/or cathodic): in this sense we have a conventional, a serpentine (SFF) or an interdigitated (IFF) flow. While the first two are sufficiently tested flow configurations, the IFF is relatively new (Fig. 3), created specifically

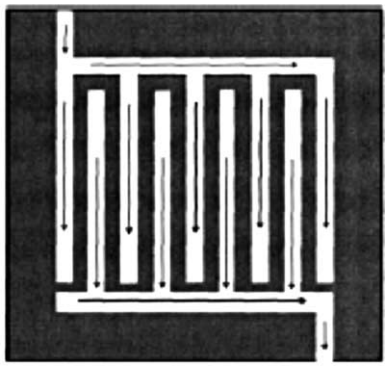

Fig. 3. Schematisation of an interdigitated flow field.

to satisfy the requirements of DMFCs. The need to overcome the problem of polarisation concentrations (more relevant in PEMFCs) and the possibility of cathodic flooding (a common drawback of DMFCs) has led to the development of this geometry for the gas distributors: the interdigitated channels are not feedthroughs (as in traditional channelled distributors) but have a "shoulder" [16].

In this way, the gases are forced to enter the electrode towards the catalytic layer to overcome this obstacle. Thus the reactant 'motion' occurs under a forced convection regime instead of a diffusion one. The diffusion layer is reduced to a thin layer close to the catalytic layer and the global kinetics increases. Furthermore, the strong tangential tension of the gas on the channel wall helps to remove a large part of the water trapped in the electrode [17].

Contrary to what may be imagined, the load losses due to forced convection are minimal: it has been demonstrated experimentally that for a "shoulder" of 1 mm, $\Delta P = 2.4$ kPa on the anodic side and 1.4 kPa on the cathodic one [16]. Thus, under a pressure of 1 bar there are load losses of 2.5% versus an increase in efficiency of 60–100%.

The second type of geometry considers the reciprocal position of the anodic and cathodic feeds: in this geometry it is possible to have three configurations, co-flow, counter-flow and cross-flow.

The calculation code provides for the possibility of choosing any possible combination of the previously described configurations (e.g. an interdigitated co-flow, a conventional counter-flow, or a serpentine cross flow, and so on), giving it the flexibility to describe different situations.

4. Results

A comparison of the results obtained with the model and literature data raises many points for discussion.

For example, Figs. 4 and 5 show the results of the simulation of a cell in an SFF co-flow configuration in a PEMFC, using the data reported in literature as input [12]: we can see that the temperature and current density maps on the cell plane are strictly correlated. In fact, in the lower part of the cell, the numerical values of the two variables are at their lowest due to the entry of the refrigerant, then they increase to reach their highest values at the entry of the reactants, when these are fresh and the water has lost part of its cooling potential, leaving room for an increase in the temperature and kinetics of the electrochemical reaction. Following such reasoning the most appropriate configuration for each particular application can be usefully discussed.

The model validation is made by fitting the experimental data collected from literature. Figs. 6 and 7 give examples of this.

Fig. 6 describes the experimental literature data on a conventional counter-flow geometry at fixed temperature [13]: it shows good agreement with the experimental data, demonstrating the reliability of the code. However, it is possible

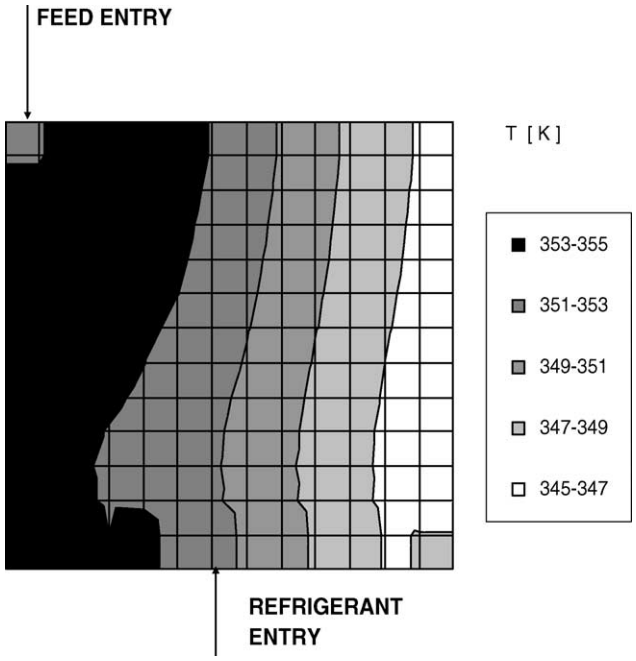

Fig. 4. PEMFC – serpentine flow field: map of temperature.

to see the search for the best Sherwood number, a very important parameter for describing the diffusion phenomena of the reagents. It is possible to note that the target value for a polymeric membrane in a conventional co-flow configuration [12] is about 0.25 (Fig. 7).

In the light of this, we have compared conventional and interdigitated cells: under the same operating conditions, the interdigitated configuration shows better performance than a

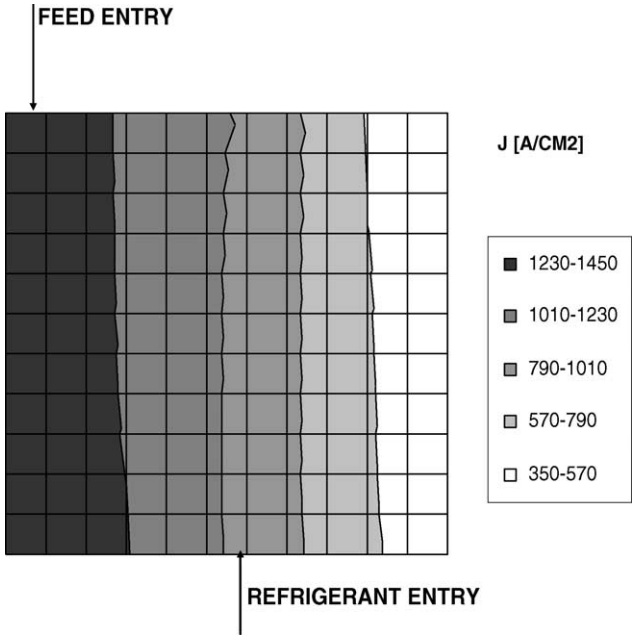

Fig. 5. PEMFC – serpentine flow field: map of current density.

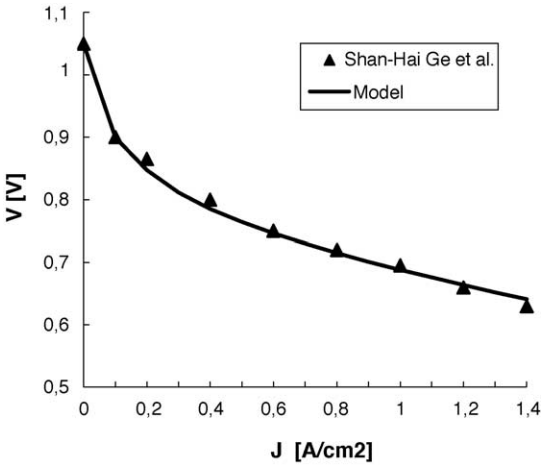

Fig. 6. PEMFC – comparison of model and experimental data for conventional counter flow.

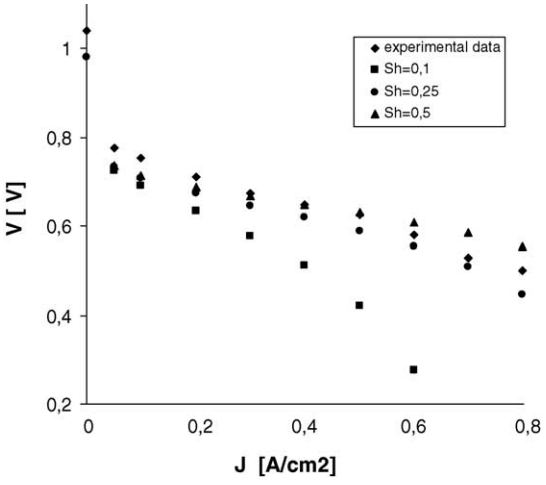

Fig. 7. PEMFC – characteristic curves varying the Sherwood number.

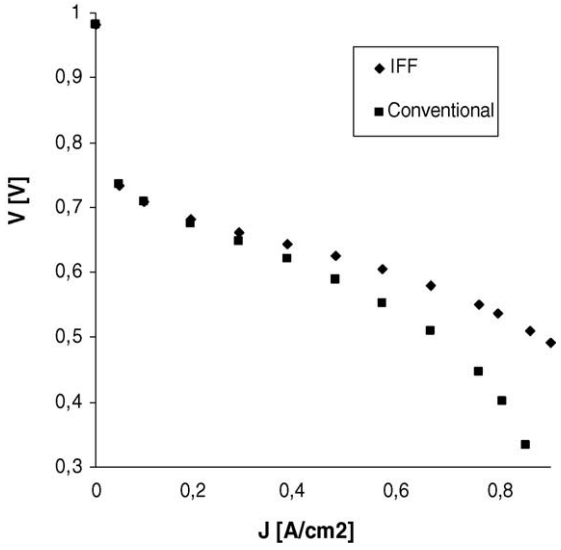

Fig. 8. PEMFC – comparison of characteristic curves for various flow geometries.

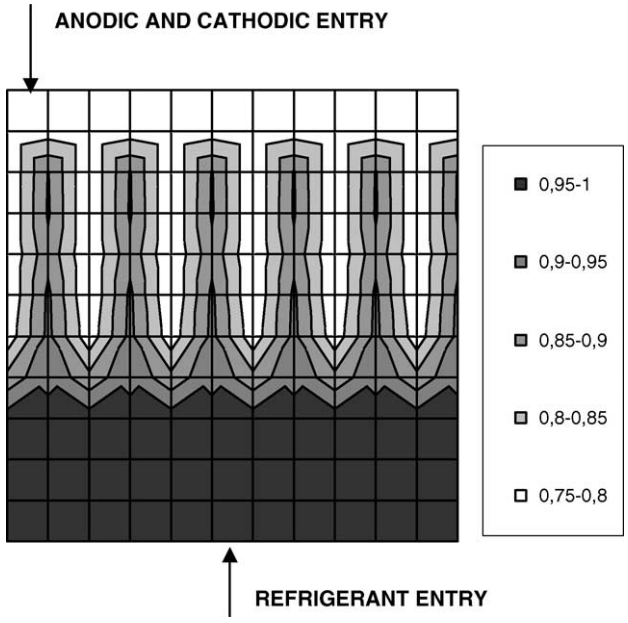

Fig. 9. PEMFC – humidity map of the cathodic side of a laboratory cell in an IFF configuration.

conventional one, especially at high current densities (Fig. 8). The improvements can be accounted for by lower resistances to diffusion (that is higher Sherwood numbers). In other words, the interdigitated configuration appears to be successful in overcoming the diffusive limits of traditional cells, so attaining higher limit currents and higher efficiency at high current densities.

Another important advantage of the interdigitated configuration is the reduction in the area where the water vapour condensation can occur on the cathodic side (Fig. 9).

Characteristic maps and curves comparing the various configurations, parametric analyses were also prepared for DMFCs and model validation carried out using the same techniques. In this case the model was calibrated on the ba-

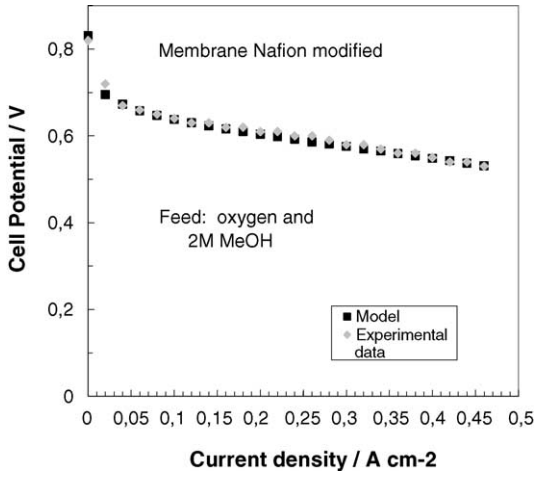

Fig. 10. DMFC – comparison of model and experimental data for conventional co-flow configuration.

sis of experimental data supplied by ITAE-CNR of Messina (Fig. 10). The agreement between the experimental data and model also seems encouraging in this case.

5. Conclusion

Although there is still ample room for improvement, especially for DMFCs, the results already obtained from simulations of low temperature fuel cells seem reliable and robust, with a satisfying agreement between experimental data and simulated values.

Future work will include more detailed study of the phenomena of water vapour condensation on the cathodic side in both PEMFCs and DMFCs, to determine what the advantages (and possible disadvantages) of the innovative interdigitated configuration are, and the study of the transport phenomena of the biphasic mix in the PEN of DMFCs.

Acknowledgments

This work has been partially supported by the Italian Department of Education, University and Research (MIUR) and the Italian National Agency for New Technologies, Energy and the Environment (ENEA) in the framework of the PRIN 2001 and FISR 2003 financed research projects, respectively. The authors would like to thank Pier Luigi Antonucci (University of Reggio Calabria, Italy) and the researchers of the Institute for Transformation and Storage of Energy (ITAE-CNR, Messina, Italy) for supplying experimental data on Direct Methanol Fuel Cells.

References

[1] M. De Francesco, E. Arato, J. Power Sources 108 (2002) 41–52.
[2] L. Li, P. Cong, R. Viswanathan, F. Qinbai, L. Renxuan, E.S. Smotkin, Electrochim. Acta 43 (1998) 3657–3663.
[3] K. Sundmacher, K. Scott, Chem. Eng. Sci. 54 (1999) 2927–2936.
[4] M. Waidhas, W. Drenckhahn, W. Preidel, H. Landes, J. Power Sources 61 (1996) 91–97.
[5] S. Hikita, K. Yamane, Y. Nakajima, JSAE Rev. 22 (2001) 151–156.
[6] A.S. Aricò, P. Cretì, V. Baglio, E. Modica, V. Antonucci, J. Power Sources 91 (2000) 202–209.
[7] K. Scott, W.M. Taama, P. Argyropoulos, J. Power Sources 79 (1999) 43–59.
[8] B. Bosio, P. Costamagna, F. Parodi, Chem. Eng. Sci. 54 (1999) 2907–2916.
[9] B. Bosio, P. Costamagna, E. Arato, P. Costa, Modeling Approach to Fuel Cell Development, Transworld Research Network, Kerala, 2002.
[10] J.H. Hirschenofer, D.B. Stauffer, R.R. Engleman, Fuel Cells. A Handbook. U.S. Department of Fossil Energy, Morgantown Energy Technology Center, Morgantown, WV, USA, 1994.
[11] K. Scott, W. Taama, J. Cruickshank, J. Power Sources 65 (1997) 159–171.
[12] P. Costamagna, Chem. Eng. Sci. 56 (2001) 323–332.
[13] S.H. Ge, B.L. Yi, J. Power Sources 124 (2003) 1–11.
[14] B. Gurau, E. Smotkin, J. Power Sources 112 (2002) 339–352.
[15] M. De Francesco, E. Arato, P. Costa, J. Power Sources 132 (2004) 127–134.
[16] J.S. Yi, T. Van Nguyen, J. Electrochem. Soc. 146 (1999) 38–45.
[17] D.L. Wood III, J.S. Yi, T. Van Nguyen, Electrochim. Acta 24 (1998) 3795–3809.